Structure of edge turbulence at plasma polarization on the CASTOR tokamak

J. Stöckel, K. Dyabilin[1], I. Ďuran, J. Horáček, M. Hron, K. Jakubka, L. Kryška,
S. Nanobashvili[2], I. Nanobashvili[2], M. Tendler[3], G. Van Oost[4], F. Žáček

Institute of Plasma Physics, Prague, Czech Republic,
[1] *High Energy Density Research Center, Inst. for High Temperatures, Moscow, Russia*
[2] *Andronikashvili Institute of Physics, Tbilisi, Republic of Georgia*
[3] *Royal Institute of Technology, Alfvén Laboratory, Stockholm, Sweden*
[4] *ERM/KMS, Laboratory for Plasma Physics, Brussels, Belgium*

Introduction: Recently, Boedo et al [1] has shown that the reduction of the fluctuation induced flux at plasma biasing is mainly due to an increase of the phase between the density and poloidal electric field fluctuations in proximity of the transport barriers. Aim of this contribution is to study impact of the sheared electric field on the spatial structure of edge fluctuations in the radial and poloidal directions. Experiments are performed on the CASTOR tokamak ($R = 0.4\ m, a = 0.085\ m$) and a biasing scheme is used to modify the radial electric field externally at the plasma edge.

Experimental arrangement: Experiments are carried at $B_t = 1\ T, I_p = 8 \div 13\ kA$ and densities $\bar{n}_e = 0.5 \div 1.5 \cdot 10^{19} m^{-3}$. The radial electric field is imposed to the edge plasma by a mushroom-like electrode biased with respect to the vacuum vessel by a pulsed voltage. The fluctuations are monitored by two multiple tip Langmuir probes arrays, oriented in the radial and poloidal directions (the spatial resolution is $2.5\ mm$) [2]. Individual tips measure either the floating potential U_{fl} or the ion saturation current I_{sat}.

Analyzed discharges are characterized by a downward shift of the plasma column, as schematically shown in Fig. 1.
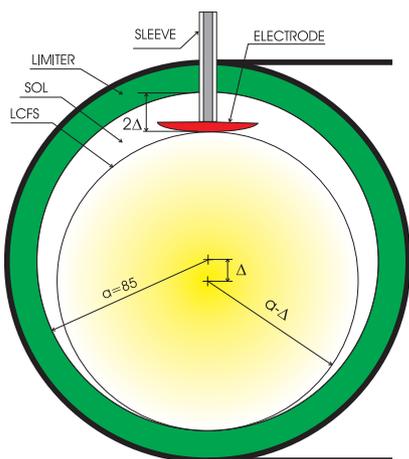

Fig. 1: Poloidal cross section, schematically showing the location of plasma column and biasing electrode.
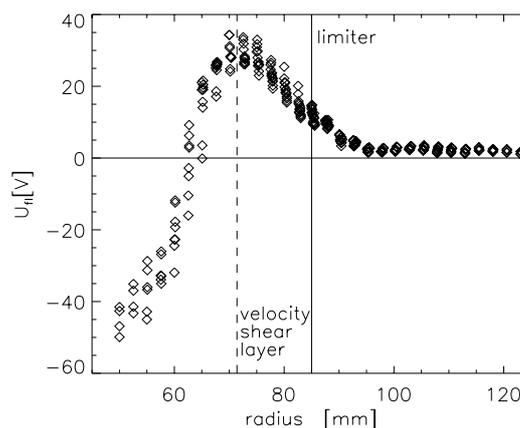

Fig. 2: Radial profile of the floating potential without biasing as measured by the radial probe array from the top of the torus. The vertical displacement is $\Delta \sim 6 \div 7\ mm$.

In the such configuration, the last closed flux surface is not already determined by the poloidal limiter. The vertical displacement is estimated from the shift of the Velocity Shear Layer (VSL),

defined here as the radius where $\nabla U_{fl} = 0$ (see Fig. 2). Due to a strong poloidal asymmetry of the scrape-off layer, the probe arrays as well as the biasing electrode are located at the top of the torus, to define better their respective positions [3]. The biasing electrode is radially located slightly outside the natural VSL and acts, in fact, as a biased limiter. Aim of this configuration is to modify the shear of the E_r in proximity of the natural VSL by positive biasing. A practical advantage of such configuration is the accessibility of the region in front of the electrode by the probe arrays.

Experimental results: The spatial/temporal evolutions of the electric field E_r and the ion saturation current I_{sat}, as measured by the radial probe array at positive biasing of the electrode are shown below.
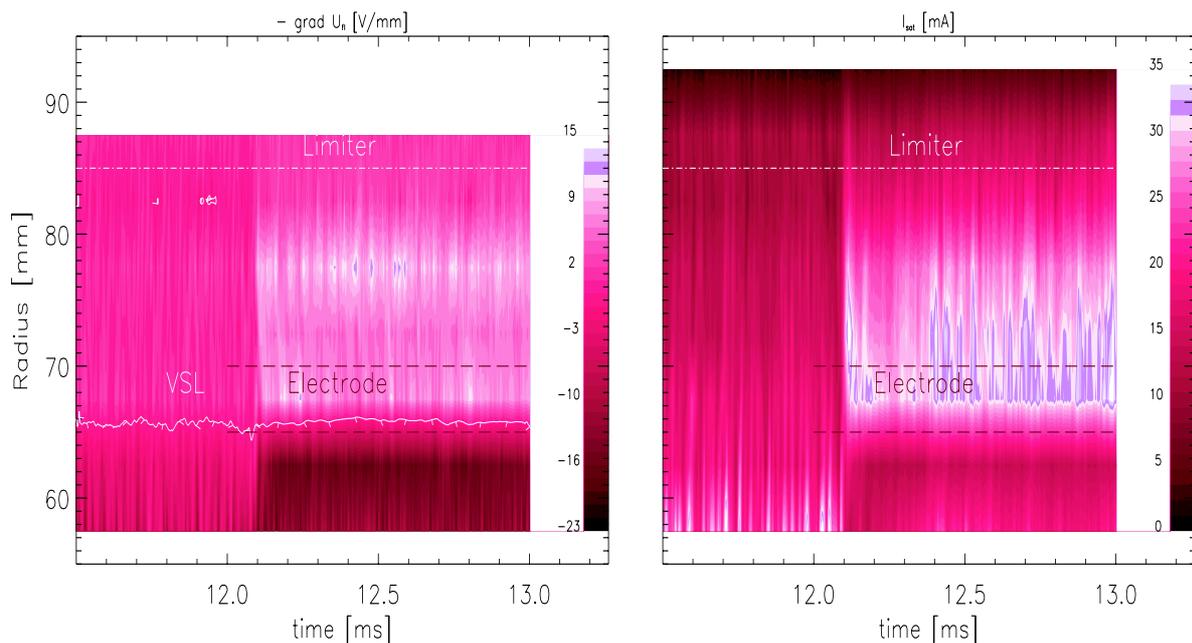

Fig. 3: Spatial-temporal evolution of the radial electric field (left) and the ion saturation current (right) at positive biasing $+200\,V$ starting at $t = 12.2\,ms$ (#7355). The radial extension od the electrode is denoted by dashed lines. The white line at $r \sim 65\,mm$ marks an instantaneous position of VSL. The spatial resolution is $5\,mm$ in this case.

It is well seen that the electric field E_r increases significantly at both the sides of the VSL, which position remains nearly unshifted. An increase of the shear dE_r/dr near VSL has a strong impact on the edge plasma, as seen from the evolution of the ion saturation current. The time average as well as the fluctuating parts of I_{sat} are significantly reduced in the confinement region ($r < r_{VSL}$) and *vice versa* (see also Fig. 4). Formation of the transport barrier [4] is followed by improvement of the global particle confinement, which is, however, less than at deeper positioning of the biasing electrode. This is probably due to strong poloidal asymmetry of the enhanced E_r-shear region.

The correlation analysis is used to deduce the characteristic dimensions/lifetimes of the turbulent structures and their propagation velocities. The poloidal length is determined, as usually, as the FWHM of the correlation function. As we show later, however, radial dimension of turbulent structures is comparable with the distance of the tips in proximity of VSL. Therefore, the correlation coefficient $C_{i,i+1}$ of signals of the adjacent tips are taken as a measure of the radial correlation length. The resulting radial profiles of these quantities are plotted in Fig. 4.
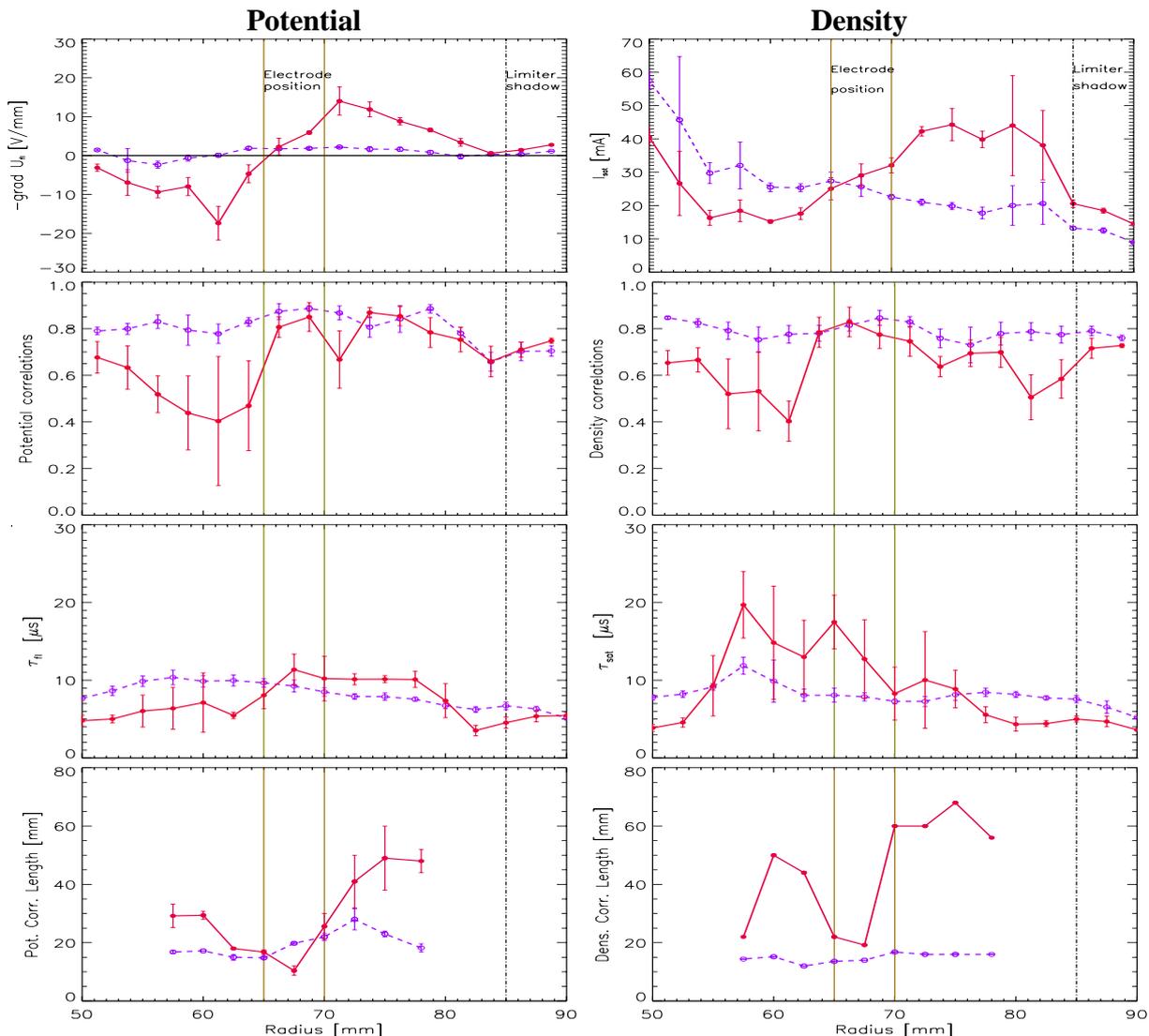
Fig. 4: Radial profiles of parameters, characterizing the potential fluctuations (left column) and density fluctuations (right column) without (dashed blue lines) and with positive biasing (full red lines). The profiles shown in the first three rows are derived using the radial probe array, while the last row corresponds to data from the poloidal probe array measured on the shot-to-shot basis.

Individual rows (from top to bottom): Time averaged radial electric field and ion saturation current, the correlation coefficient $C_{i,i+1}$ of signals of adjacent tips (proportional to the radial correlation length), the autocorrelation time (determined as the FWHM of the autocorrelation function) and the poloidal correlation length.

At biasing, the E_r—shear at the separatrix increases significantly by a factor of 5 (from 0.8 to $4\,V/mm^2$). The response of the edge turbulence is quite complex, as evident from the figures. A dramatic drop of the potential as well as density correlation coefficients $C_{i,i+1}$ is observed in the region, where E_r appears to be more negative, i.e. in the confinement region. On the other hand, fluctuations seem to be radially "untouched" within the scrape-off layer ($E_r > 0$). One should note that the drop of $C_{i,i+1}$ below 0.5 implies a reduction of the radial correlation length below 2.5 mm. The observed reduction of the autocorrelation time, observed at $E_r < 0$ for potential fluctuation and at $E_r > 0$ for density fluctuation can be explained either by a reduction of the

life time of fluctuations or due to an enhanced poloidal rotation (a Doppler shift). However, an increase of τ_a, observed at particular radii, can be attributed only to an increase of average lifetime of turbulent structures. The poloidal correlation length increases with biasing at both sides of the electrode.

The fluctuation-induced flux Γ and the averaged phase shift of the n- and E_r-fluctuations can be deduce using data from the poloidal probe array (see Fig. 5). The radial profile of the poloidal phase velocity of fluctuations is plotted for comparison.
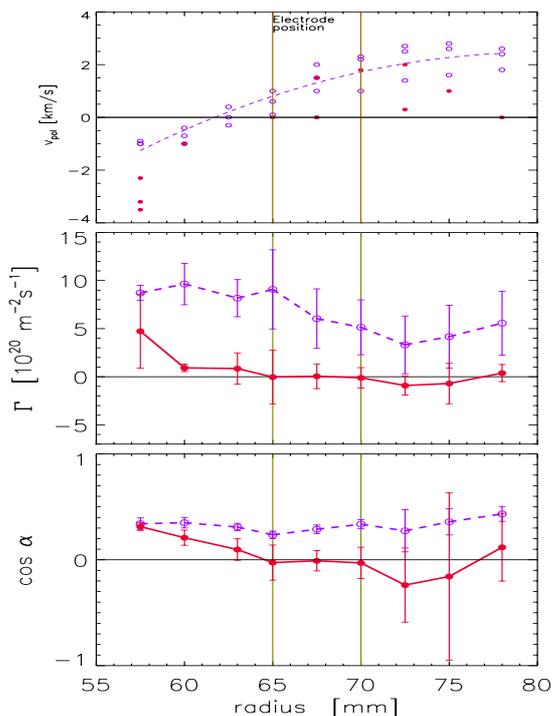

Fig. 5: Radial profile of the poloidal velocity v_{pol}, fluctuation-induced flux Γ and the phase angle between the density and poloidal electric field fluctuations.

As seen, the fluctuation-induced flux

$$\Gamma = < \delta n \delta E_p > /B_t$$

is suppressed outside the VSL, mainly due to the increase of the phase between the density and poloidal field fluctuations [1]:

$$\cos \alpha = < \delta n \delta E_p > /\sqrt{< \delta n^2 >< \delta E_p^2 >}$$

(levels of fluctuations are not reduced more than by a factor of 2).

Conclusions: The enhanced shear of the radial electric field in the separatrix region in polarized discharges impacts dramatically on the edge electrostatic fluctuations. Some observed features, such as the radial decorrelation in proximity of VSL, can be expected. However, the observed increase of the poloidal correlation and lifetime of fluctuations is not yet understood. The last effects could be related to a quasiperiodic low frequency component ($f \leq 10 \ kHz$) of plasma fluctuations, which appears during biasing (seen in Fig. 3). Such modulation is even more apparent, if the electrode is deeper in the edge plasma and biased to more than $+150V$.

It is evident that the correct interpretation of such complex behaviour requires additional experiments.

References

[1] J. Boedo, G. Van Oost et al: Czech. J. Phys., 48(1998),12, Suppl. S2, p. 99

[2] J. Stöckel et al: Plasma Phys. Control. Fusion, 41, (1999), A577-A585

[3] For more details see http://www.ipp.cas.cz/tokamak/castor/recent.htm

[4] M. Tendler: Plasma Phys. Control. Fusion, 39, (1997), B371-B382